Author/s:
Collins, SJ;Haigh, CL

Title:
Simplified Murine 3D Neuronal Cultures for Investigating Neuronal Activity and Neurodegeneration

Date:
2017-03-01

Citation:
Collins, S. J. & Haigh, C. L. (2017). Simplified Murine 3D Neuronal Cultures for Investigating Neuronal Activity and Neurodegeneration. Cell Biochemistry and Biophysics, 75 (1), pp.3-13. https://doi.org/10.1007/s12013-016-0768-z.

Persistent Link:
https://hdl.handle.net/11343/216780

Simplified murine 3D neuronal cultures for investigating neuronal activity and neurodegeneration

Collins SJ. Haigh CL.*

Department of Medicine (Royal Melbourne Hospital)

Melbourne Brain Centre

The University of Melbourne

30 Royal Parade

Parkville

Melbourne

Victoria 3010

Australia

Tel. +61 3 8344 1952

E-mail. chaigh@unimelb.edu.au

Keywords: Neural stem cell, neurobiology, 3D, differentiation, prion

The ability to model brain tissue in three-dimensions (3D) offers new potential for elucidating functional cellular interactions and corruption of such functions during pathogenesis. Many protocols now exist for growing neurones in 3D and these vary in complexity and cost. Herein, we describe a straight-forward method for generating terminally differentiated central nervous system (CNS) cultures from adult murine neural stem cells. The protocol requires no specialist equipment, is not labour intensive or expensive and produces mature cultures within 10 days that can survive beyond a month. Populations of functional glutamatergic neurones could be identified within cultures. Additionally, the 3D neuronal cultures can be used to investigate tissue changes during the development of neurodegenerative disease where demonstration of hallmark features, such as plaque generation, has not previously been possible using two-dimensional cultures of neuronal cells. Using a prion model of acquired neurodegenerative disease, biochemical changes indicative of prion pathology were induced within 2-3 weeks in the 3D cultures. Our findings show that tissue differentiated in this simplified 3D culture model is physiologically competent to model CNS cellular behaviour as well as manifest the functional failures and pathological changes associated with neurodegenerative disease.

Introduction

The architecture of the brain is complex, demonstrating intricately organised neuronal pathways and networks. The structure conferred on cells by their environmental scaffold governs their functioning and limits how cells receive signals from and react in response to signals from their surrounding cells and environment [1]. Such complexity has posed many problems for modelling brain tissue *in vitro* but overcoming this obstacle is necessary if our understanding of the functional pathways of the brain and its degeneration during disease are to be adequately understood.

Methods and matrices for growing neurones in three-dimensional (3D) cultures have existed for over twenty years [2, 3]. Being able to generate 3D cultures of neurones has recognised advantages in the laboratory, including understanding cellular communications networks, diffusion of molecules through tissue and 'clinical trials in a dish' technology [4, 5]. Recently new applications of 3D culture techniques have been extensively developed for growing neurones in 3D with the aim of reproducing tissue architecture such that function and disease can be explored with minimal need for tissue harvests [6, 7].

It is now well established that the adult brain contains neural stem cells (NSCs), which have a limited capacity to replace brain cells throughout life [8-11]. NSCs can self-renew and are multipotent; they can differentiate into cells of any CNS lineage. NSCs can be harvested from mouse brain tissue and cultures expanded under standard incubator conditions, making them a plentiful source of cells for 3D differentiation into CNS tissue [12]. Furthermore, the potential to generate 3D cultures from existing transgenic mouse lines permits use of their respective gene manipulations for investigation of gene function or dysfunction.

Many 3D culture systems have been investigated in recent years; some make use of specifically engineered biopolymers [13, 14], some use natural matrix scaffolds [15, 16], some use chip technology [17-19] and some utilise scaffold-free suspension culture [6]. Each has it benefits and limitations, and researcher choice can often be guided by factors such as budget and time commitment. Whilst major caveats in all systems include the lack of vascularisation and structural limitations imposed by the skull, the use of neurones grown in 3D is one step closer to reproducing functioning brain tissue. Herein we describe a simple and inexpensive system for generating functional 3D neuronal cultures from murine NSCs with minimal outlay, no specialist equipment and little manipulation by the researcher.

Methods

Neural stem cell harvest and culture

Neural stem cells (NSCs) were harvested from the brains of 3 mice at 8 weeks of age as previously described [20]. NSCs were routinely grown as neurospheres in complete proliferation medium (Stem Cell Technologies, VIC, AUS), supplemented with final concentrations of 10 ng/ml FGF, 20 ng/ml EFG and 2 μg/ml heparin, at 37°C in a humidified, 5% CO2 tissue culture incubator. Proliferating neurospheres were maintained in Nunc uncoated flasks (Thermo Fisher Scientific, AUS) to avoid adhesion to the plastic surface. Neurospheres were mechanically passaged every 5-8 days as judged by their diameter and were not allowed to become necrotic at the core. Medium was replenished using a half exchange as often as required to prevent acidification.

2D differentiation

Eight-well chambered coverslips were coated with poly-D lysine (Sigma-Aldrich, NSW, AUS) for a minimum of one hour at room temperature and washed once with phosphate buffered saline (PBS, -Ca/-Mg pH7.2; Gibco, Thermo Fisher Scientific) immediately prior to plating. Plates were not permitted to dry out during this procedure. NSCs were collected by centrifugation at 100 ×g for 5 mins, brought into single cell suspension by mechanical dissociation and washed once in PBS, followed by further centrifugation at 150 ×g for 5 mins, before resuspending in an appropriate volume of complete differentiation medium (Stem Cell Technologies). Cells were seeded at a density of 8×10^4 cells/well and returned to a standard tissue culture incubator for 10 days differentiation, with a half media exchange every three days.

3D differentiation

Neurospheres were grown to ~150-200 μm in diameter but were not allowed to become necrotic (darkened) within their core. Up to 50 neurospheres were washed in PBS and transferred into 2 ml of differentiation medium per well of an uncoated polystyrene 6-well culture plate (Corning Costar, Sigma-Aldrich). Plates were placed on a rotational mixer at 85 rpm in a standard tissue culture incubator and incubated for 48 hours with agitation, then removed from the mixer for 24 hours static culture, after which time they resumed agitation as before. Media was exchanged, as a half exchange, every three days.

Immunofluorescent staining of 2D cultures

Fixing and staining of 2D monolayers has been described previously [21, 22]. Antibodies and concentrations were as described for 3D immuno-staining.

Fixing and lipid clearance of 3D cultures

Fixing and staining of the 3D cultures was carried out in 8-well chambered coverslip slides (Nunc, Thermo Fisher Scientific). Wells were filled with 300 μl of sterile PBS before transferring cells. For each 3D culture, the pipette tip was cut with sterile scissors to create a wide enough aperture that the 3D culture would not be damaged by shearing forces and 100 μl of media containing the 3D cultures was transferred to the 300 μl of PBS already in the well. Cultures were washed twice more by aspirating half of the PBS and replacing the same volume. For each wash, aspirating from near the cultures was avoided to ensure they were not damaged and the slide was mildly agitated by tapping to mix. Following the final wash, 200 μl of PBS were aspirated from each well and 200 μl of an 8 % (w/v) paraformaldehyde solution added to

fix the cells. Fixation was allowed to proceed for 1 hour for small diameter cultures (<2 mm) and 2 hours for large (>2 mm) cultures. Following fixation cultures were washed five times by aspirating half of the fixative/wash and replacing it with a fresh equal volume (200 µl) as before, being careful not to damage the cultures. Half of the PBS from the well (200 µl) was removed and replaced with 200 µl of 2 × sodium dodecyl sulfate (SDS) permeabilisation buffer (2% [w/v] SDS, 0.2 M boric acid, pH 8) resulting in a final 1% [w/v] SDS/0.1 M boric acid buffer. Cultures were permeabilised at room temperature first for 15 minutes in the 1% [w/v] SDS buffer then, following exchange of half of the well volume (200 µl) with fresh PBS, in 0.5% [w/v] SDS for a further 30 mins. Cultures were washed five times using half volume exchanges of PBS.

Immunofluorescent staining of 3D cultures

Blocking was carried out in 10% [v/v] foetal bovine serum (FBS), 1% [w/v] bovine serum albumin (BSA, Sigma-Aldrich) in PBS for 1 hour at room temperature. Blocking buffer was diluted by a half volume exchange with PBS then aspirated completely, taking care not to damage the culture with the pipette tip. Antibodies were applied in 1% [v/v] FBS, 1% [w/v] BSA in PBS at the following concentrations: Neuro Filament-L (NF-L, Thermo Fisher Scientific) 1 in 50; glial fibriliary acidic protein (GFAP, Stem Cell Technologies) 1 in 100; NMDA receptor subunit-2B (NR2B, Abcam, AUS) 1 in 50; nestin (Sigma-Aldrich) 1 in 50; doublecortin (DCX, Abcam) 1 in 100; and PrP (03R19, kind gift from Victoria Lawson [23]) 1 in 100. Cultures were incubated for 48 hrs at 4°C in a humidified chamber. Following primary antibody incubation, the entire antibody solution was aspirated with care and cultures were washed 3× using half volumes PBS exchanges. The final PBS solution was aspirated entirely before addition of secondary antibody. Secondary antibodies, anti-rabbit Alexa Fluor 488 and

anti-mouse Alexa Fluor 647 (Thermo Fisher Scientific), were added diluted 1 in 250 in 1% [v/v] FBS, 1% [w/v] BSA in PBS and slides were incubated overnight at 4°C in the dark. Cultures were washed after secondary antibody incubation as for primary antibodies and then were mounted in 3-4 drops of mounting media with DAPI (Sigma-Aldrich). A pipette tip was used to position the culture within the well then mounting medium was cured overnight at room temperature before imaging.

Confocal imaging

Confocal imaging was carried out using a Leica SP8 confocal microscope as described in [24]. Z-projections were generated using Fiji (ImageJ 1.50d) imaging software [25]. Images shown are representative of cultures generated from >3 independent differentiations unless otherwise stated.

Caspase imaging

The manufacture and characterisation of the NIR-VAD-fmk probe have been described previously [26]. Live cultures were incubated with 2.5 μM NIR-VAD-fmk for 30 minutes then imaged using a Nikon Eclipse TE2000-E epi-fluorescence microscope (Nikon-Roper Scientific, Coherent Scientific, AUS). Following imaging cultures were transferred to fresh media for continued incubation. Image analysis was done using NIS-Elements imaging software (Nikon-Roper Scientific).

Calcium influx assay

Cultures were collected by centrifugation at 100 × g for 5 mins. Using a cut pipette tip, 3-4 organoids per well were transferred into a 96-well plate in 100 μl of fresh differentiation

medium. Using the Fluo-4 Direct™ Calcium Assay Kit (Thermo Fisher Scientific), at the beginning of the assay 100 µl of calcium assay working buffer, prepared as per manufacturer's instructions, was added to each test well. Plates were incubated for one hour with readings taken using 488 nm excitation and 530 nm emission filters in a FluoSTAR Optima (BMG Labtech, AUS), the basal rate of calcium influx was calculated once a linear relationship was stable. After basal calcium flux had been determined 10 mM glutamate (Sigma-Aldrich) was added and readings taken for a further two hours. Rates were calculated as linear tangents to the curve using MARS analysis software (BMG Labtech).

Prion infections

Brain homogenates from M1000 prion strain [27] infected and sham inoculated, 'mock' infected mice were prepared as a 10% (w/v) stock in PBS. Prion infection was induced within the 3D cultures by including infected and mock homogenates in normal culture media at a final concentration of 0.01% (w/v) for 72-hours.

Thioflavin-T (ThT) staining

Cultures were incubated in normal media containing 10 µM ThT (Sigma-Aldrich) with agitation for 30 minutes before fixing as described above.

Results and Discussion

Morphology of cultures differentiated in 3D; Three-dimensional cultures of CNS tissue were generated using neurospheres of murine NSCs that had been grown to the size limit of the culture (~150-200 μm) without being allowed to become necrotic at their core. Using the principle of culture agitation previously described for generating 3D cultures of neuronal cells [15], at induction of differentiation neurospheres were constantly stirred by orbital mixing followed by a static period and then further agitated incubation. The experimental protocol is shown in Figure 1A. Two dimensional cultures reach maturity (as detected by markers of mature neurones) by 7 days' differentiation. Since the cores of the 3D cultures were not accessible to the differentiation medium, and so diffusion of signals would need to occur from the sphere surface, differentiation was allowed to proceed for several days longer (to 10 days) before assessment of the cellular populations. Visual inspection of the cultures indicated that once maturity was reached they did not continue to expand in size neither did they shrink with age in the time period considered. Figure 1B shows brightfield morphology of 3D cultures. Immunostaining for neurones and astrocytes demonstrated an outer astrocytic layer, wrapping around the culture with a denser neuronal stratum underneath (Fig 1C). The neuronal:astrocytic ratio of the cells could be influenced towards neurones by including 1 μg/ml laminin in the culture medium during differentiation (Fig 1D).

Crude structural formations were observed, with protuberances reminiscent of lobes budding from the periphery of the cultures and regions of overlaid dense cells. Some of the structural formations appeared to be due to the agitation causing distension of culture boundaries and some looked as if due to several cultures fusing together and wrapping around each other, with neurones appearing to line up along the interfaces. It was apparent that agitation was required

for the structural adhesion of cultures as those differentiated in non-agitated suspension cultures were fragile, breaking apart on manipulation (data not shown).

Comparison of cell populations within 2D and 3D cultures shows increased neuronal differentiation in 3D; To determine how successful the differentiation of the 3D cultures had been as compared with neuronal populations achievable in 2D differentiations, parallel cultures were differentiated in 2D and 3D (without additional laminin) for 10 days and compared for markers of NSCs (nestin; Fig 2A), neural precursors (DCX; Fig 2B) and mature neurones (NF-L); expression profiles relative to neuronal maturity are shown in Fig 1A. Qualitative assessment of the staining intensity indicated that greater neuronal signal is observed in the 3D cultures. This observation is consistent with human 3D culture systems that also report increased neuronal content over 2D differentiation [28]. In 3D cultures immature cells are localised nearer the surface of the culture rather than throughout as seen in the 2D cultures. Visual inspection shows that the most immature NSCs (nestin positive) are most externally located, with the neuroblasts (DCX positive) located as a layer between nestin and the NF-L stained mature neurones. As compared with the 2D differentiations, the 3D cultures display less nestin staining but comparatively more DCX indicating that less of the cells cultured in 3D have failed to differentiate and more have committed to neuronal lineage. The external localisation of the nestin-positive NSCs is alongside the region where GFAP was detected and, whilst the staining pattern differs between the GFAP and nestin antibodies, there may be some GFAP staining of the cultures that is due to expression of GFAP in immature NSCs. Since no further expansion of the cultures was observed following differentiation, the immature cells on the periphery of the culture might be senescent, quiescent awaiting specific growth/differentiation signals, incapable of differentiation or performing an as yet unknown function for the maintenance of the culture.

Production of neuronal subsets within the 3D cultures; For the 3D cultures to be useful models they must demonstrate cell functionality. To consider whether functional neuronal subsets were being produced within the culture, the activity of glutamatergic neurones was measured by calcium flux prior to and following stimulation with glutamate. Significant calcium influx was observed upon glutamate challenge (Fig 3A), indicating functional glutamatergic neurones reside within the cultures. For visualisation of glutamatergic neurones, cultures were stained for expression of the NMDA receptor subunit 2B (NR2B). The staining showed strong signal mostly towards the periphery of the culture with some dense areas inside the core (Fig 3B).. Contour intensity plots were generated for comparison of the positioning of the glutamatergic neurones with the other cellular subsets within the culture. Regions of interest were gated at the periphery of the culture (Fig 4A) and within the core (Fig 4B). These plots show a clear, narrow nestin positive region at the outer edge of the culture. Inside of this was a layer of astrocytes/GFAP-positive cells and neuronal precursors intermingled with mature neurones, including the glutamatergic neurones. The neurones extended further into the tissue and only neurones were detected within the core, with small puncta of glutamatergic staining. The layer summary schematic is shown in Fig 4C.

Cultures survive for up to 6 weeks; To determine culture longevity and the reasonable window for experimentation, cellular attrition in the 3D cultures was monitored over time. The cultures were incubated with a near-infra-red (NIR), pan-caspase imaging probe at 1, 3 and 6 weeks following culture induction (Fig 5A-C). A NIR probe was employed in these assays because when neuronal tissue degenerates lypofuscin is produced, which fluoresces through the green-red wavelength range and can mask the genuine signal from many imaging probes [26]. Caspase probe intensity was monitored relative to autofluorescence background (Fig 5D) and very low

uptake of the pan-caspase probe was observed at three weeks (Fig 5B) with the staining pattern diffuse, indicative of background binding. Attrition of the culture, seen as punctate staining of individual cells within localised regions became apparent at 6 weeks (Fig 5C).

Induction of a neurodegenerative disease phenotype; A particular advantage to 3D neuronal cultures is the possibility of modelling neurodegenerative diseases, which often have hallmark features that cannot be detected in 2D monolayer cultures even of primary neurones. To determine whether the 3D neuronal cultures could develop disease pathology we induced a neurodegenerative disease phenotype.

Prion diseases are transmissible neurodegenerative diseases. The transmissibility of prion diseases offers an advantage for the study of neurodegeneration as infection (and therefore neurodegeneration) can be transmitted from culture to culture. However, very few secondary cell lines show overt abnormalities or monitorable prion pathology, instead displaying only propagation of the protein agent. NSCs cultures have previously been shown to have utility as models of prion infection. NSCs can propagate prions both when growing and following differentiation into mature CNS cells [29, 30]. Furthermore, using our NSC model, toxic changes are seen in differentiated neurones and astrocytes when exposed to prions [20, 22]. Prion infection was induced within the 3D cultures by a single 72-hour exposure to the M1000 prion strain [27] from infected mouse brain homogenates (0.01% [w/v] final concentration), with normal, uninfected brain homogenates used to treat 'mock' control cultures. Three weeks post-infection, cultures were fixed and stained to look for changes in their neuronal/astrocytic morphology. No overt change could be seen in the neuronal population; however astrocytes surrounding the infected culture exterior appeared to show reduced GFAP staining and displayed altered morphology (Fig 6).

Reduced detection of astrocytes appears contrary to the astrocytosis reported in prion disease, however, there may be a number of factors contributing to the reduced staining such as: expression of PrP in astrocytes changes their isoform expression profiles [21] and this may also occur upon infection, changing GFAP detection; three weeks may be too short a time period to detect astrocyte proliferation; astrocytes play a role in re-modelling the extra-cellular matrix during times of disease or stress [31] and this could result in changes of astrocytic adhesion, which, in the absence of the structure imposed by the dense CNS neuropil and extracellular matrix interstitium, might cause these cells to be lost into the surrounding media; the astrogliosis associated with prion disease also involves the recruitment of microglia [32], which stimulate astrocyte proliferation [33] and in the absence of their signals the astrocytes may not be stimulated to grow - further co-culture experiments will be required to assess this role (note that microglia do not differentiate from NSCs but are derived from the bone marrow and so should not be present in our cultures). Further, during human prion disease hypertrophic astrocytes show two morphologies, glial fibril containing and a subset showing suboptimal fixation resulting in a "watery" cytoplasm appearance [34] - the astrocytes in the 3D cultures may be the latter subset resulting in apparently reduced GFAP detection. Finally, astrocytes die following astrogliosis in certain forms of brain injury [35-37] and, in the case of our 3D cultures, the infection (accumulation of prions [38] and markers of cell damage [39] are known to occur in astrocytes) may have tipped astrocytes from a helpful response to cell death. These unknowns further demonstrate the potential information that can be ascertained by assaying CNS cells in 3D rather than monolayer culture.

Cell death in the brains of prion infected mice, as shown by caspase activation, can be detected in neurones residing within the hippocampus and thalamus, and is found in close proximity to

PrP deposition [40]. To assess if prion infection results in accelerated culture death, cultures were imaged following incubation with the NIR pan-caspase probe at 8, 15 and 22 days post infection (dpi) to determine if the culture was displaying prion-induced cell death. Significantly more caspase puncta were observed in the cultures exposed to prions than those receiving the mock treatment and this was obvious by 15 dpi and dramatically increased by 22 dpi (Fig 7A). A heat map of capase activation at 22 dpi shows that very little caspase activation occurs within the outer layer of the culture but regions of heightened activation arise through the mixed layer and extends into the neuronal core (Fig 7B). The 22 dpi cultures were fixed for immunostaining either with (Fig 7C) or without incubation with thioflavin-T (ThT) to identify deposits of aggregated protein. Cultures without ThT staining were incubated with antibodies against the prion protein (PrP) to directly identify PrP deposits (Fig 7D). Examination of the cultures showed deposits of PrP replicating plaque formation. PrP detection was increased in the infected cultures, which is observed as mis-folded PrP accumulates both human disease and animal models of disease [41, 42]. Comparison with 3D cultures generated from prion knock-out NSCs showed that the PrP detected is not due to persistence of the original inoculums (Sup Fig 1). The ThT-positive aggregates and PrP-staining deposits were lying within neuron-dense regions of the culture and also alongside the boarders of these regions, which may represent formation at the periphery of the neuronal population or within regions too dense for the antibody staining to penetrate (Fig 7C/D). A further observation was that DAPI staining became less distinct in the infected cultures suggesting that the nuclear material may be breaking down as part of the toxicity of infection.

The formation of ThT-reactive protein deposits shows that the mechanisms impaired in the brain during neurodegenerative diseases are equally affected when neurones are cultured in 3D and

therefore the 3D cultures can be used to examine these failures *in vitro*. This could have potential applications for investigating other neurodegenerative diseases where plaque formation is a hallmark, such as Alzheimer's Disease (AD). As NSCs can be harvested from the brain of any mouse, transgenic AD mouse models could be utilised to make these cultures for such research. Validations of potential therapeutics targeting mitigation of protein deposition can be examined in this system for their capacity to prevent or clear protein deposits before human *in vivo* trial. Furthermore, the ease of their production and relatively minimal time scales to produce cultures permit many validations to be performed quickly and cheaply.

Conclusions

Growing neurones from NSCs in 3D offers a number of advantages over traditional primary cultures. Herein, we developed a neuronal 3D culture system that was relatively inexpensive and time efficient. NSCs can be harvested from the brains of adult mice or from developing embryos. Therefore, NSC lines can be made containing any mutation that can be engineered into a mouse. Ethical, logistical and cost advantages to using these cells include that they can be expanded to produce differentiated cultures on demand and cryopreserved for longevity, thereby reducing the numbers of mice needed for harvests, the time taken for repeated harvests and the costs of maintaining mouse colonies. Our simple and relatively inexpensive approach for growing murine CNS tissue in 3D produces cultures with good longevity that can be used to study neuronal function. It further offers a system for investigating the pathogenesis and biochemical pathways of disease that cannot be studied in 2D and a potential model for therapeutic compound screening, wherein changes in 3D readouts may more reliably reproduce changes observed *in vivo*.

Acknowledgements

This work was funded by an NHMRC program grant (SJC, #628946) and an NHMRC project grant (CLH, #APP1044264). SJC is supported by an NHMRC Practitioner Fellowship (#APP100581) and CLH is supported by a CJDSGN Memorial Grant in memory of Rhonda McCoy and the many people affected by prion disease in Australia.

References

1. Bard, J. and T. Elsdale, *Growth regulation in multilayered cultures of human diploid fibroblasts: the roles of contact, movement and matrix production.* Cell Tissue Kinet, 1986. **19**(2): p. 141-54.
2. Bellamkonda, R., et al., *Hydrogel-based three-dimensional matrix for neural cells.* J Biomed Mater Res, 1995. **29**(5): p. 663-71.
3. Justice, B.A., N.A. Badr, and R.A. Felder, *3D cell culture opens new dimensions in cell-based assays.* Drug Discov Today, 2009. **14**(1-2): p. 102-7.
4. Haston, K.M. and S. Finkbeiner, *Clinical Trials in a Dish: The Potential of Pluripotent Stem Cells to Develop Therapies for Neurodegenerative Diseases.* Annu Rev Pharmacol Toxicol, 2015.
5. Lai, Y., K. Cheng, and W. Kisaalita, *Three dimensional neuronal cell cultures more accurately model voltage gated calcium channel functionality in freshly dissected nerve tissue.* PLoS One, 2012. **7**(9): p. e45074.
6. Pasca, A.M., et al., *Functional cortical neurons and astrocytes from human pluripotent stem cells in 3D culture.* Nat Methods, 2015.
7. Terrasso, A.P., et al., *Novel scalable 3D cell based model for in vitro neurotoxicity testing: Combining human differentiated neurospheres with gene expression and functional endpoints.* J Biotechnol, 2015. **205**: p. 82-92.
8. Emsley, J.G., et al., *Adult neurogenesis and repair of the adult CNS with neural progenitors, precursors, and stem cells.* Prog Neurobiol, 2005. **75**(5): p. 321-41.
9. Kitabatake, Y., et al., *Adult neurogenesis and hippocampal memory function: new cells, more plasticity, new memories?* Neurosurg Clin N Am, 2007. **18**(1): p. 105-13, x.

10. Lugert, S., et al., *Quiescent and active hippocampal neural stem cells with distinct morphologies respond selectively to physiological and pathological stimuli and aging.* Cell Stem Cell, 2010. **6**(5): p. 445-56.

11. Wang, Y.Z., et al., *Concise review: Quiescent and active states of endogenous adult neural stem cells: identification and characterization.* Stem Cells, 2011. **29**(6): p. 907-12.

12. Ahlenius, H. and Z. Kokaia, *Isolation and generation of neurosphere cultures from embryonic and adult mouse brain.* Methods Mol Biol, 2010. **633**: p. 241-52.

13. Bosi, S., et al., *From 2D to 3D: novel nanostructured scaffolds to investigate signalling in reconstructed neuronal networks.* Sci Rep, 2015. **5**: p. 9562.

14. Lu, H.F., et al., *Efficient neuronal differentiation and maturation of human pluripotent stem cells encapsulated in 3D microfibrous scaffolds.* Biomaterials, 2012. **33**(36): p. 9179-87.

15. Lancaster, M.A. and J.A. Knoblich, *Generation of cerebral organoids from human pluripotent stem cells.* Nat Protoc, 2014. **9**(10): p. 2329-40.

16. Labour, M.N., et al., *3D compartmented model to study the neurite-related toxicity of Abeta aggregates included in collagen gels of adaptable porosity.* Acta Biomater, 2016.

17. Anene-Nzelu, C.G., et al., *Scalable alignment of three-dimensional cellular constructs in a microfluidic chip.* Lab Chip, 2013. **13**(20): p. 4124-33.

18. Moreno, E.L., et al., *Differentiation of neuroepithelial stem cells into functional dopaminergic neurons in 3D microfluidic cell culture.* Lab Chip, 2015. **15**(11): p. 2419-28.

19. Seidel, D., et al., *Induced tauopathy in a novel 3D-culture model mediates neurodegenerative processes: a real-time study on biochips.* PLoS One, 2012. **7**(11): p. e49150.

20. Haigh, C.L., et al., *Acute exposure to prion infection induces transient oxidative stress progressing to be cumulatively deleterious with chronic propagation in vitro.* Free Radic Biol Med, 2011. **51**(3): p. 594-608.

21. Collins, S.J., et al., *The prion protein regulates beta-amyloid mediated self-renewal of neural stem cells in vitro.* Stem Cell Res Ther, 2015. **6**(1): p. 60.

22. Sinclair, L., et al., *Cytosolic caspases mediate mislocalised SOD2 depletion in an in vitro model of chronic prion infection.* Dis Model Mech, 2013. **6**(4): p. 952-63.

23. Lawson, V.A., et al., *Mouse-adapted sporadic human Creutzfeldt-Jakob disease prions propagate in cell culture.* Int J Biochem Cell Biol, 2008. **40**(12): p. 2793-801.

24. Haigh, C.L., A.R. McGlade, and S.J. Collins, *MEK1 transduces the prion protein N2 fragment antioxidant effects.* Cell Mol Life Sci, 2015. **72**(8): p. 1613-29.

25. Schindelin, J., et al., *Fiji: an open-source platform for biological-image analysis.* Nat Meth, 2012. **9**(7): p. 676-682.

26. Lawson, V.A., et al., *Near-infrared fluorescence imaging of apoptotic neuronal cell death in a live animal model of prion disease.* ACS Chem Neurosci, 2010. **1**(11): p. 720-7.

27. Brazier, M.W., et al., *Correlative studies support lipid peroxidation is linked to PrP(res) propagation as an early primary pathogenic event in prion disease.* Brain Res Bull, 2006. **68**(5): p. 346-54.

28. Choi, S.H., et al., *A three-dimensional human neural cell culture model of Alzheimer's disease.* Nature, 2014. **515**(7526): p. 274-8.

29. Herva, M.E., et al., *Prion infection of differentiated neurospheres.* J Neurosci Methods, 2010. **188**(2): p. 270-5.

30. Milhavet, O., et al., *Neural stem cell model for prion propagation.* Stem Cells, 2006. **24**(10): p. 2284-91.

31. Jones, E.V. and D.S. Bouvier, *Astrocyte-secreted matricellular proteins in CNS remodelling during development and disease.* Neural Plast, 2014. **2014**: p. 321209.

32. Marella, M. and J. Chabry, *Neurons and astrocytes respond to prion infection by inducing microglia recruitment.* J Neurosci, 2004. **24**(3): p. 620-7.

33. Brown, D.R., *Microglia and prion disease.* Microsc Res Tech, 2001. **54**(2): p. 71-80.

34. Liberski, P.P. and P. Brown, *Astrocytes in transmissible spongiform encephalopathies (prion diseases).* Folia Neuropathol, 2004. **42 Suppl B**: p. 71-88.

35. Takuma, K., A. Baba, and T. Matsuda, *Astrocyte apoptosis: implications for neuroprotection.* Prog Neurobiol, 2004. **72**(2): p. 111-27.

36. Szydlowska, K., M. Zawadzka, and B. Kaminska, *Neuroprotectant FK506 inhibits glutamate-induced apoptosis of astrocytes in vitro and in vivo.* J Neurochem, 2006. **99**(3): p. 965-75.

37. Saas, P., et al., *CD95 (Fas/Apo-1) as a receptor governing astrocyte apoptotic or inflammatory responses: a key role in brain inflammation?* J Immunol, 1999. **162**(4): p. 2326-33.

38. Diedrich, J.F., et al., *Scrapie-associated prion protein accumulates in astrocytes during scrapie infection.* Proc Natl Acad Sci U S A, 1991. **88**(2): p. 375-9.

39. Andreoletti, O., et al., *Astrocytes accumulate 4-hydroxynonenal adducts in murine scrapie and human Creutzfeldt-Jakob disease.* Neurobiol Dis, 2002. **11**(3): p. 386-93.

40. Drew, S.C., et al., *Optical imaging detects apoptosis in the brain and peripheral organs of prion-infected mice.* J Neuropathol Exp Neurol, 2011. **70**(2): p. 143-50.

41. Meyer, R.K., et al., *Separation and properties of cellular and scrapie prion proteins.* Proc Natl Acad Sci U S A, 1986. **83**(8): p. 2310-4.

42. Muramoto, T., et al., *The sequential development of abnormal prion protein accumulation in mice with Creutzfeldt-Jakob disease.* Am J Pathol, 1992. **140**(6): p. 1411-20.

Figure Legends

Figure 1. *Differentiation and morphology of neuronal 3D cultures*. **A.** Schematic of the 3D differentiation protocol and expression of cellular markers during maturation. **B.** Examples of culture size and morphology, presented in wells of a 24-well plate. Well diameter is indicated and red arrows and brackets indicate the position of cultures of varying size. Immunofluorescent staining of whole cultures differentiated without (**C**) or with 1 µg/ml laminin (**D**) in the differentiation medium. A selection of individual stack channels and merges are shown as z-projections. Neurones are labelled by NF-L (red) staining, astrocytes by GFAP (green) and cell nuclei by DAPI (blue) uptake. Scale bars = 50 µm.

Figure 2. *Comparison of cellular maturity between 2D and 3D cultures.* Cultures were differentiated in 2D and 3D for 10 days as per the respective differentiation protocols and immature cells detected with antibodies against (**A**) nestin (green) and **(B)** doublecortin (DCX; green) as compared with mature neurones (NF-L). Cell nuclei are labelled with DAPI (blue). Scale bar = 100 µm.

Figure 3. *Culture function*. **A**. Calcium influx assay comparing culture response before and after stimulation with glutamate. Graph shows mean and s.e.m. of the rates. Students t-test, t = 3.134, n = 4.**B**. Immunofluorescent staining of glutamatergic neurones in the culture detected using the NMDA receptor subunit 2B (NR2B; green). Nuclei are stained with DAPI in blue. Scale bar = 100 µm.

Figure 4. *Culture layers.* Intensity contour plots of (**A**) culture periphery and (**B**) culture core for comparison of marker distribution. Nestin, GFAP, DCX and NR2B are shown in green, DAPI in blue and NF-L in red. **C**. Schematic of culture layer composition.

Figure 5. *Culture viability.* Cultures were incubated with NIR-VAD-fmk pan-caspase probe at 1 (**A**), 3 (**B**) and 6 (**C**) weeks post-differentiation. **D**. Background fluorescence of the culture in the absence of probe collected under identical imaging conditions. Scale bar = 100 μm.

Figure 6. *Morphology of 3D cultures following exposure to prions.* Cultures were incubated for 22 days following exposure to infectious prion or mock control brain homogenate and stained for neuronal and astrocytic content. For each, two magnifications are shown (upper panels scale bar = 100 μm / lower panels scale bar = 20 μm) with channels split into nuclei (DAPI; blue), astrocytes (GFAP; green) and neurones (NF-L; red) alongside the merged image as indicated.

Figure 7. *3D cultures develop a prion neurodegenerative phenotype*. **A**. Culture death, as shown by incubation with the pan-caspase probe NIR-VAD-fmk, indicates accelerated attrition in the cultures exposed to prion infection. **B.** Heat plot of regions of heightened caspase activation extending into the tissue from the culture surface. Intensity scale is shown right. **C**. Incubation of cultures with ThT (cyan) at 22 dpi and immunofluorescent staining for neurones

(NF-L; red; left panels scale bar = 100 µm, right upper and lower scale bar = 50 µm, right middle panel scale bar = 20 µm). Cell nuclei are stained with DAPI (blue). **D**. Immunofluorescent staining of cultures at 22 dpi for PrP (green) and NF-L (red; nuclei shown with DAPI in blue) shows increased PrP staining and punctate deposits in the infected cultures. Scale bars = 50 µm. Representative images are shown from 4 independent differentiations in A and 2 each of these were used for staining in C and D.

<?xml version="1.0" encoding="UTF-8" ?>
<funding-group>
<award-group id="ID0EP5AE778">
<funding-source funder-id="http://dx.doi.org/10.13039/501100000925">National Health and Medical Research Council</funding-source>
<award-id>APP1044264</award-id>
<principal-award-recipient>
<principal-award-recipient-first-name>Cathryn</principal-award-recipient-first-name>
<principal-award-recipient-last-name>L Haigh</principal-award-recipient-last-name>
<orcid verified="yes">0000-0001-7591-1149</orcid>
</principal-award-recipient>
</award-group>
<award-group id="ID0ETEAG779">
<funding-source funder-id="http://dx.doi.org/10.13039/501100000925">National Health and Medical Research Council</funding-source>
<award-id>628946</award-id>
<principal-award-recipient>
<principal-award-recipient-first-name>Steven</principal-award-recipient-first-name>
<principal-award-recipient-last-name>Collins</principal-award-recipient-last-name>
</principal-award-recipient>
</award-group>
<award-group id="ID0E6FAG780">
<funding-source funder-id="http://dx.doi.org/10.13039/501100000925">National Health and Medical Research Council</funding-source>
<award-id>APP100581</award-id>
<principal-award-recipient>
<principal-award-recipient-first-name>Steven</principal-award-recipient-first-name>
<principal-award-recipient-last-name>Collins</principal-award-recipient-last-name>
</principal-award-recipient>
</award-group>
<award-group id="ID0ELHAG781">
<funding-source funder-id="">Philanthropic donation</funding-source>
<principal-award-recipient>
<principal-award-recipient-first-name>Cathryn</principal-award-recipient-first-name>
<principal-award-recipient-last-name>L Haigh</principal-award-recipient-last-name>
<orcid verified="yes">0000-0001-7591-1149</orcid>
</principal-award-recipient>
</award-group>
</funding-group>

A.

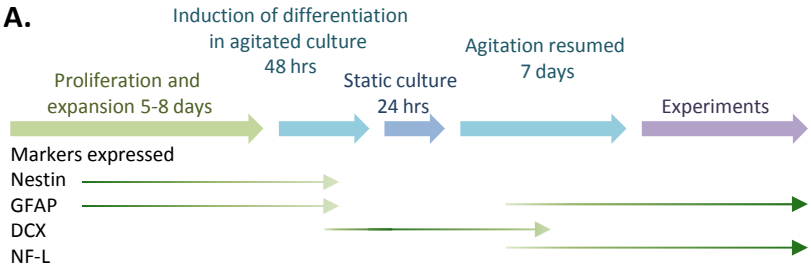

B.

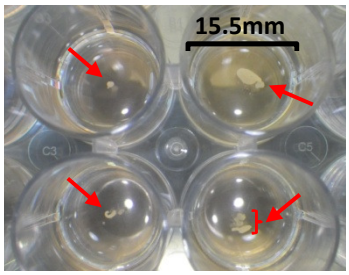

C. Normal differentiation medium.

Single Z-stack slices | Z projection

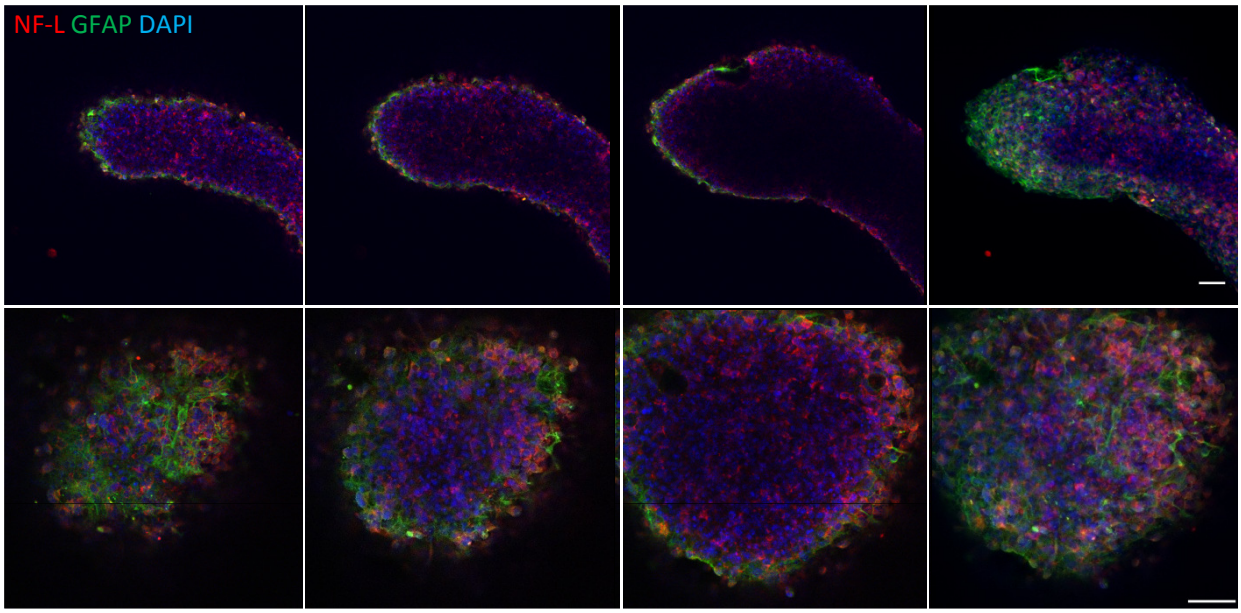

D. Differentiation medium plus 1 µg/ml laminin.

Single Z-stack slices | Z projection

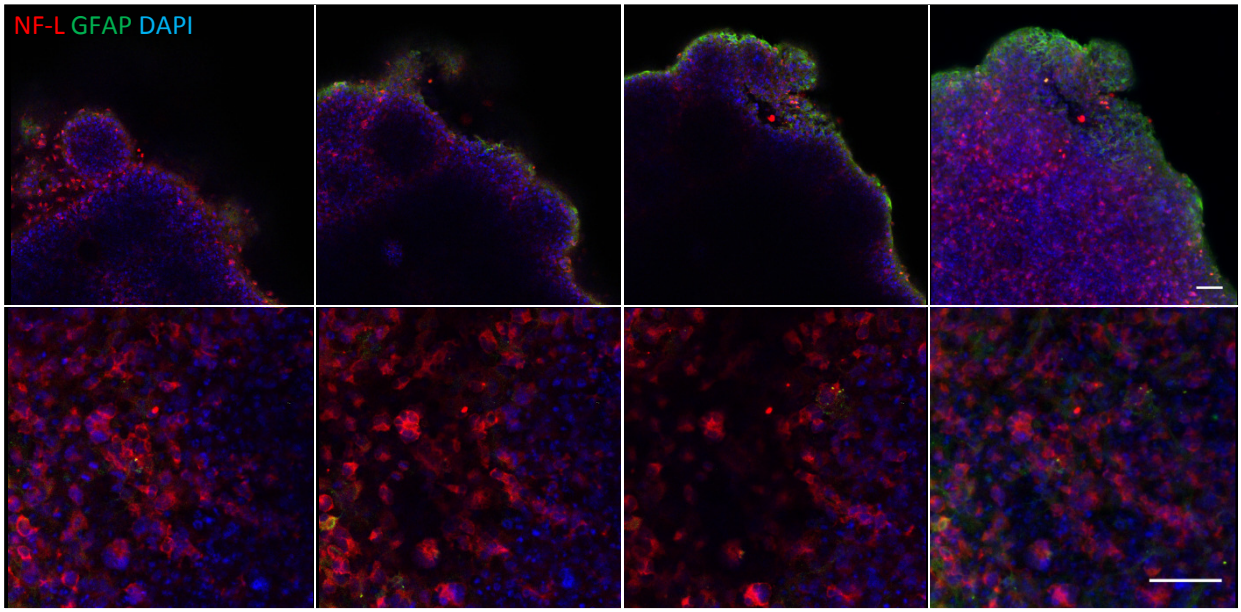

Collins & Haigh, Figure 1

A.

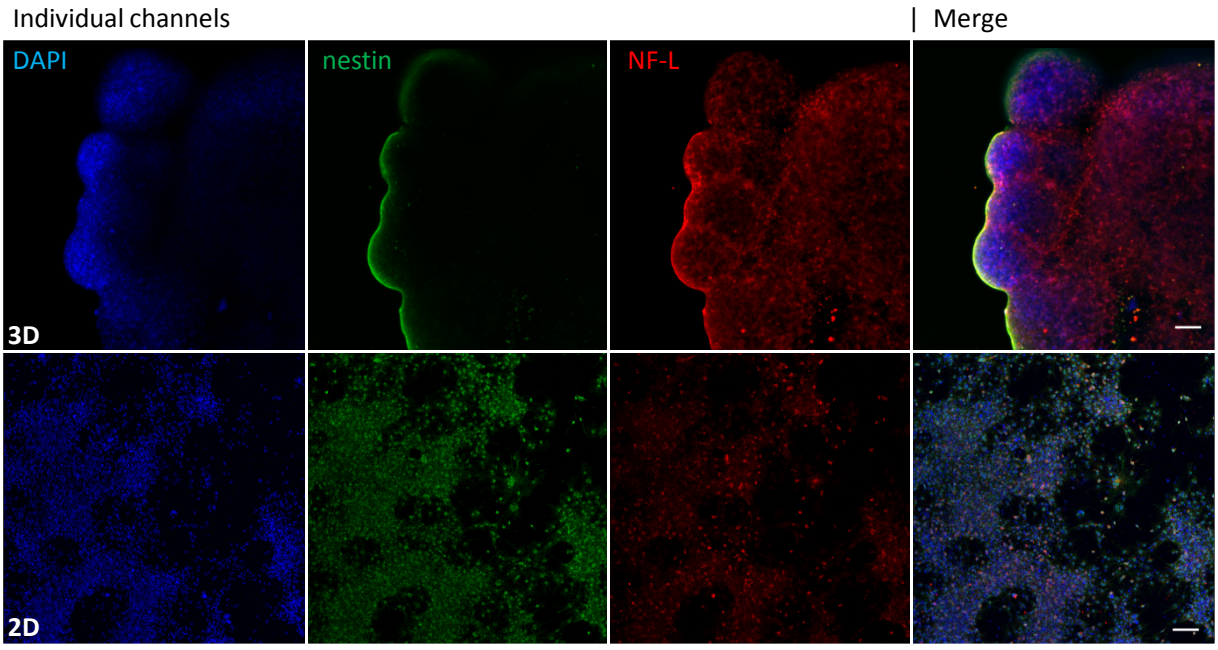

B.

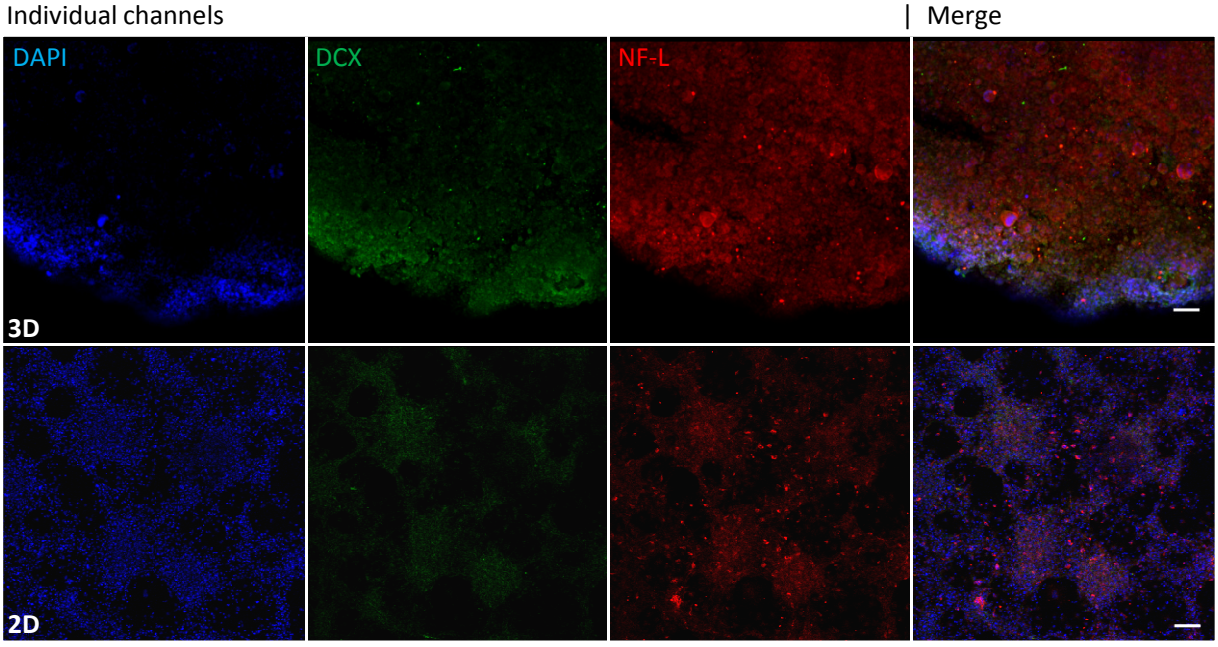

Collins & Haigh, Figure 2

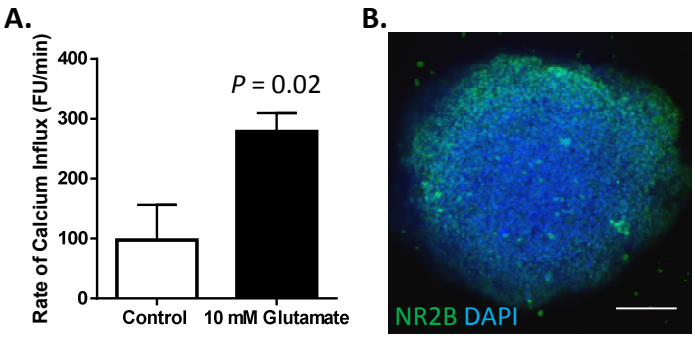

Collins & Haigh, Figure 3

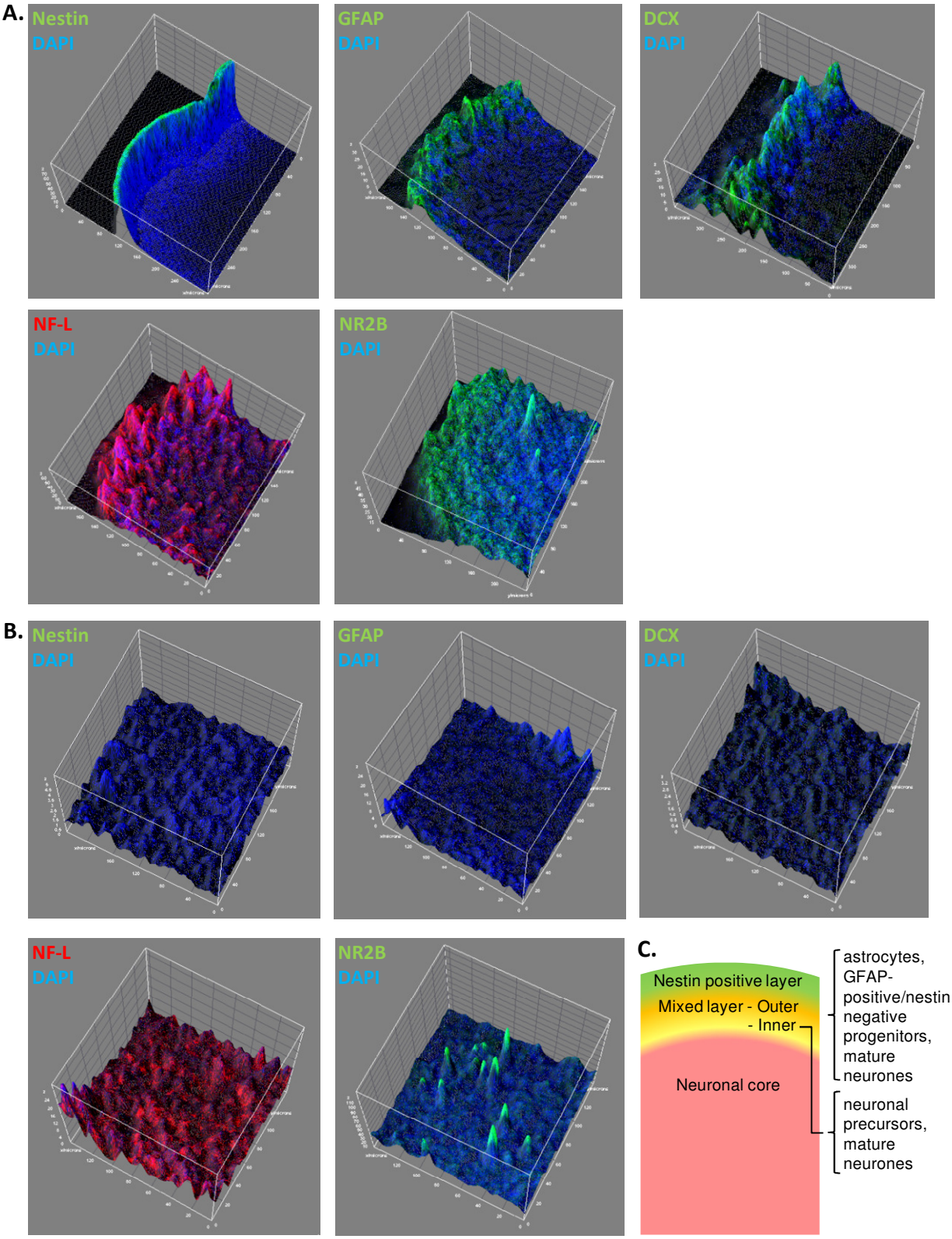

Collins & Haigh, Figure 4

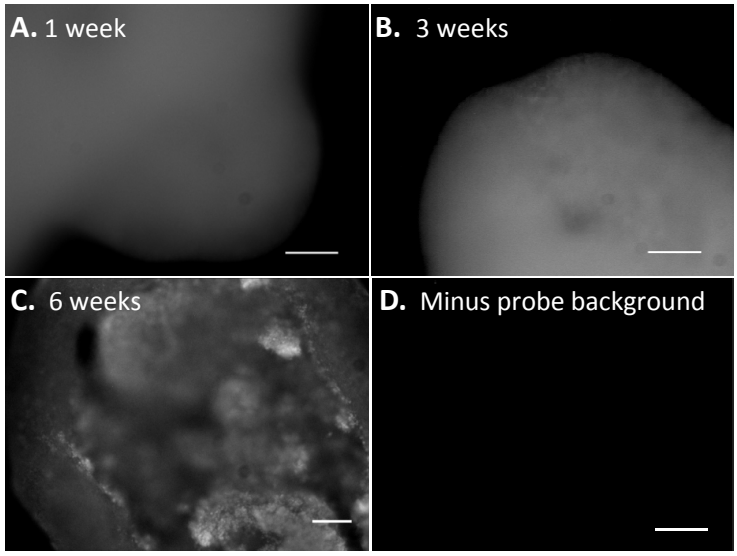

Collins & Haigh, Figure 5

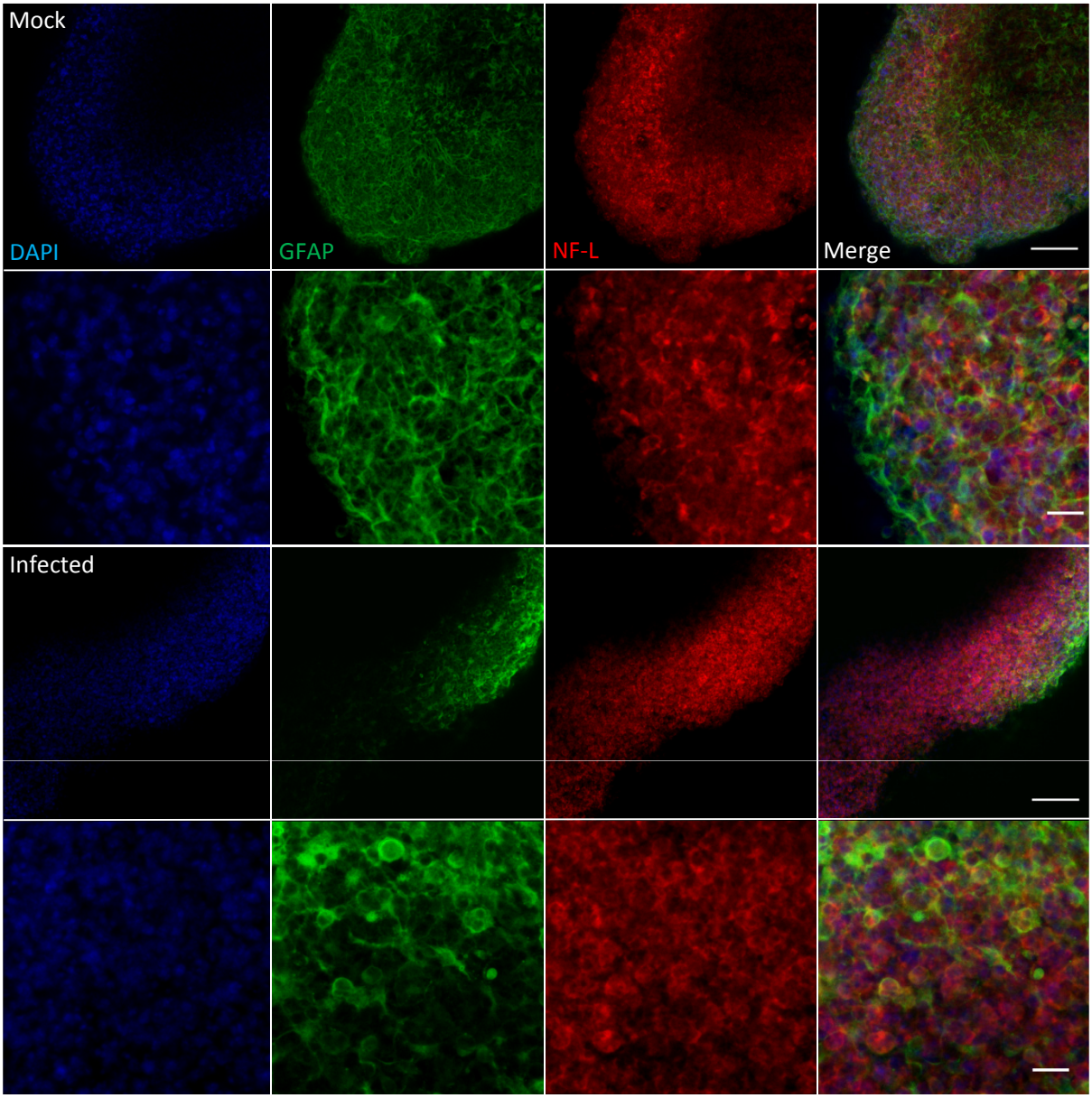

Collins & Haigh, Figure 6

A.

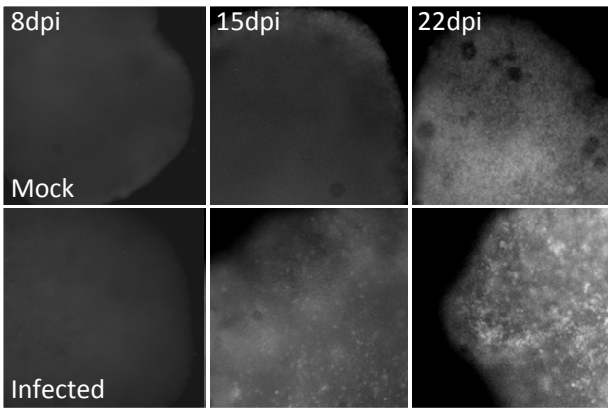

B. Infected 22 dpi.

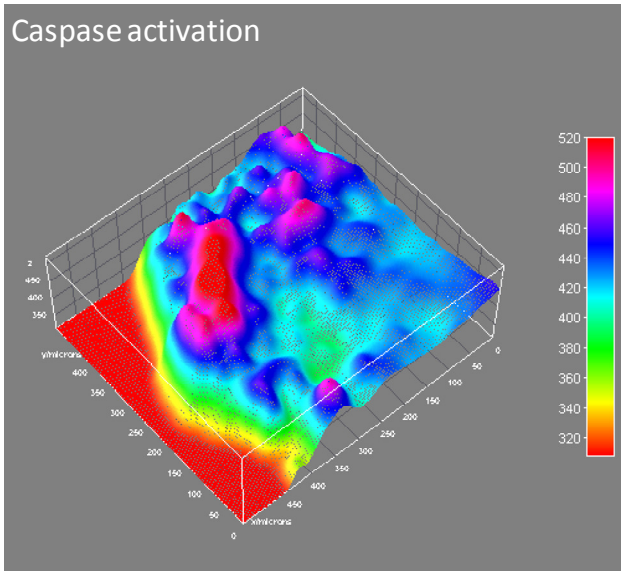

C.

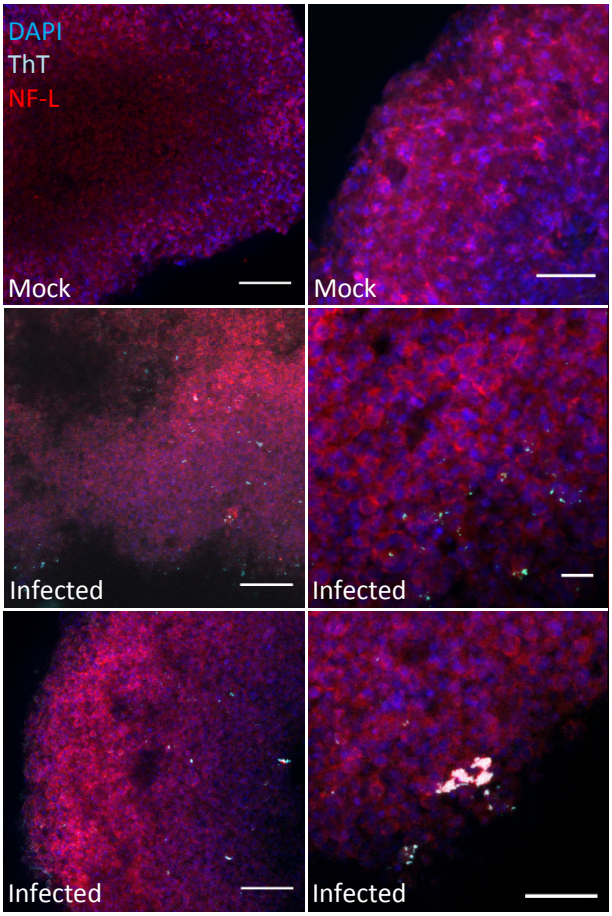

D.

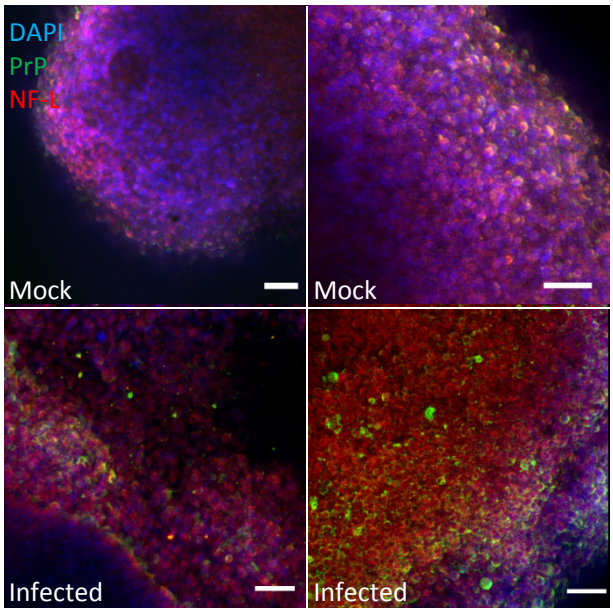

Collins & Haigh, Figure 7

Supplementary Figure 1. *PrP detection in mock and infected prnp knock-out cultures.* 3D cultures were generated from *prnp* knock-out NSCs [1]. Cultures were treated with mock and infected inoculums exactly as described for the wild type cultures. Three weeks post infection cultures were fixed and immunofluorescently labelled for PrP (red) and DAPI (blue). Scale bar = 100 µm. No residual PrP signal was detected from either the mock or infectious inoculum and no deposits were detected indicative of the inoculum forming plaques deposits that could not be digested by the culture. This indicates the wild type infected cultures that accumulate PrP and the plaques within these cultures are caused by prion propagation rather than an inability to clear the inoculum. A caveat to comparing the knock-out cultures with the wild type infections is that we, like others [2-5], see significant differences between the behaviours of the cells (growth and differentiation) that is dependent upon PrP expression [6]. These PrP-dependent differences influence the cellular composition of the starting culture and many fewer neurones are seen in the 3D cultures generated from knock-out NSCs. Such variations are not a problem when comparing mock and infected wild type cells that are generated from the same starting culture.

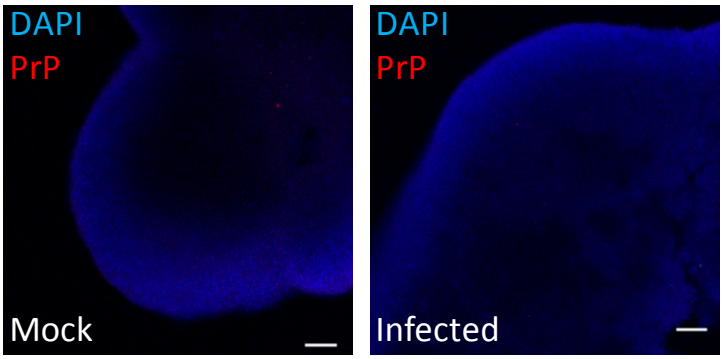

1. Haigh, C.L., et al., *Acute exposure to prion infection induces transient oxidative stress progressing to be cumulatively deleterious with chronic propagation in vitro.* Free Radic Biol Med, 2011. **51**(3): p. 594-608.
2. Santos, T.G., et al., *Enhanced neural progenitor/stem cells self-renewal via the interaction of stress-inducible protein 1 with the prion protein.* Stem Cells, 2011. **29**(7): p. 1126-36.
3. Peralta, O.A., W.R. Huckle, and W.H. Eyestone, *Expression and knockdown of cellular prion protein (PrPC) in differentiating mouse embryonic stem cells.* Differentiation, 2011. **81**(1): p. 68-77.
4. Steele, A.D., et al., *Prion protein (PrPc) positively regulates neural precursor proliferation during developmental and adult mammalian neurogenesis.* Proc Natl Acad Sci U S A, 2006. **103**(9): p. 3416-21.
5. Bribian, A., et al., *Role of the cellular prion protein in oligodendrocyte precursor cell proliferation and differentiation in the developing and adult mouse CNS.* PLoS One, 2012. **7**(4): p. e33872.
6. Collins, S.J., et al., *The prion protein regulates beta-amyloid mediated self-renewal of neural stem cells in vitro.* Stem Cell Res Ther, 2015. **6**(1): p. 60.